Article

Characterization of Mg^{2+} Binding to the DNA Repair Protein Apurinic/Apyrimidic Endonuclease 1 via Solid-State ^{25}Mg NMR Spectroscopy

A. S. Lipton, R. W. Heck, S. Primak, D. R. McNeill, D. M. Wilson III, and P. D. Ellis

J. Am. Chem. Soc., **2008**, 130 (29), 9332-9341 • DOI: 10.1021/ja0776881 • Publication Date (Web): 25 June 2008

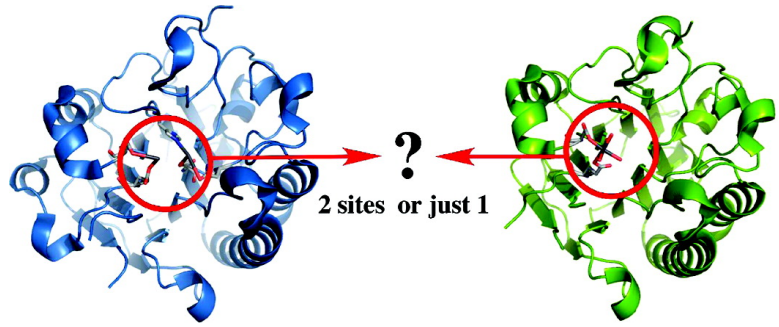

More About This Article

Additional resources and features associated with this article are available within the HTML version:

- Supporting Information
- Access to high resolution figures
- Links to articles and content related to this article
- Copyright permission to reproduce figures and/or text from this article

View the Full Text HTML

J|A|C|S
ARTICLES

Published on Web 06/25/2008

Characterization of Mg^{2+} Binding to the DNA Repair Protein Apurinic/Apyrimidic Endonuclease 1 via Solid-State ^{25}Mg NMR Spectroscopy

A. S. Lipton,[†] R. W. Heck,[†] S. Primak,[†] D. R. McNeill,[‡] D. M. Wilson III,[*,‡] and P. D. Ellis[*,†]

The Biological Sciences Directorate, Pacific Northwest National Laboratory, K8-98, 902 Battelle Boulevard, Richland, Washington 99352, and Laboratory of Molecular Gerontology, GRC, National Institutes on Aging, IRP, National Institutes of Health, 5600 Nathan Shock Drive, Baltimore, Maryland 21224-6825

Received October 5, 2007; E-mail: paul.ellis@pnl.gov

Abstract: Apurinic/apyrimidinic endonuclease 1 (APE1), a member of the divalent cation-dependent phosphoesterase superfamily of proteins that retain the conserved four-layered α/β-sandwich structural core, is an essential protein that functions as part of base excision repair to remove mutagenic and cytotoxic abasic sites from DNA. Using low-temperature solid-state ^{25}Mg NMR spectroscopy and various mutants of APE1, we demonstrate that Mg^{2+} binds to APE1 and a functional APE1−substrate DNA complex with an overall stoichiometry of one Mg^{2+} per mole of APE1 as predicted by the X-ray work of Tainer and co-workers (Mol, C. D.; Kuo, C. F.; Thayer, M. M.; Cunningham, R. P.; Tainer, J. A. *Nature* **1995**, *374*, 381−386). However, the NMR spectra show that the single Mg^{2+} site is disordered. We discuss the probable reasons for the disorder at the Mg^{2+} binding site. The most likely source of this disorder is arrangement of the protein−ligands about the Mg^{2+} (cis and trans isomers). The existence of these isomers reinforces the notion of the plasticity of the metal binding site within APE1.

Introduction

Nuclear DNA is continuously damaged by endogenous sources, such as reactive oxygen species produced during normal cellular respiration, or by exogenous sources, such as ionizing radiation.[1] It has been estimated that over 10 000 DNA lesions are produced in *each* cell every day.[2] Because genomic preservation is critical to an organism's health and survival,[3] a variety of DNA repair pathways, such as base excision repair (BER), nucleotide excision repair (NER), and DNA mismatch repair (DMR), have evolved to recognize and repair genomic damage. The bulk of DNA lesions produced by both oxidative stress and ionizing radiation in cells are oxidized bases (e.g., 8-oxoguanosine, 8OG), single-strand breaks, and sites of base loss, which are in turn substrates for the BER pathway. While the overwhelming majority of DNA lesions are repaired, the consequence of damage *not* being repaired is carcinogenesis, aging, and genetic disease.[1,4] Hence, DNA repair is essential for life.[5]

BER plays a critical role in preventing the cytotoxic and mutagenic effects of most spontaneous alkylation and oxidative DNA damage. We concentrate herein on a single protein that is central to the BER pathway: the apurinic/apyrimidic (AP) endonuclease 1 (APE1), which shows sequence and structural homology to the divalent cation-dependent phosphoesterase superfamily of proteins that maintain a conserved four-layered α/β-sandwich structural core.[6] APE1 recognizes AP sites in DNA that arise either spontaneously or as enzymatic products of DNA repair glycosylases that excise substrate base lesions as part of the BER response.[7,8] Subsequent to damage recognition, the chemistry central to the function of APE1 is water-activated by a magnesium ion followed by hydrolytic cleavage of the phosphodiester bond immediately 5′ to the abasic site. Magnesium binding to APE1 is an absolute requirement for this endonucleolytic activity, which ultimately permits removal of the abasic moiety and gap-filling by DNA polymerase β.[9,10]

APE1 is a 35.5 kDa protein that, as described above, initiates repair of abasic sites in damaged DNA and also functions in the excision of 3′-oxidative DNA damage (e.g., 3′-phosphates) and 3′-mismatched nucleotides.[11,12] There are six crystal structures (PDB accession codes 1BIX, 1DE8, 1DE9, 1DEW, 1HD7, and 1E9N) of APE1, where nearly all employed

[†] Pacific Northwest National Laboratory.
[‡] NIH.

(1) Friedberg, E. C.; Walker, G. C.; Siede, W. In *DNA Repair and Mutagenesis*; American Society for Microbiology: Washington, DC, 1995; pp 283−365.
(2) Ames, B. N.; Shigenaga, M. K.; Hagen, T. M. *Proc. Natl. Acad. Sci. U.S.A.* **1993**, *90*.
(3) Lindahl, T.; Wood, R. D. *Science* **1999**, *286*.
(4) Cleaver, J. E.; Kraemer, K. H. *The Metabolic Basis of Inherited Disease*; McGraw-Hill Book Co.: New York, 1989.
(5) Wilson, D. M., III; Thompson, L. H. *Proc. Natl. Acad. Sci. U.S.A.* **1997**, *94*, 12754–12757.
(6) Schien, C. H.; Ozgun, N.; Izumi, T.; Braum, W. *BMC Bioinf.* **2002**, *25*, 37.
(7) Wilson, D. M.; Barsky, D. *Mutat. Res.* **2001**, *485*, 283–307.
(8) Demple, B.; Sung, J. S. *DNA Repair* **2005**, *4*, 1442–1449.
(9) Erzberger, J. P.; Wilson, D. M. *J. Mol. Biol.* **1999**, *290*, 447–457.
(10) Beard, W. A.; Wilson, S. A. *Mutat. Res.* **2000**, *460*, 231.
(11) Chou, K. M.; Cheng, Y. C. *Nature* **2002**, *415*, 655–659.
(12) Wilson, D. M. *J. Mol. Biol.* **2003**, *330*, 1027–1037.

10.1021/ja0776881 CCC: $40.75

Scheme 1

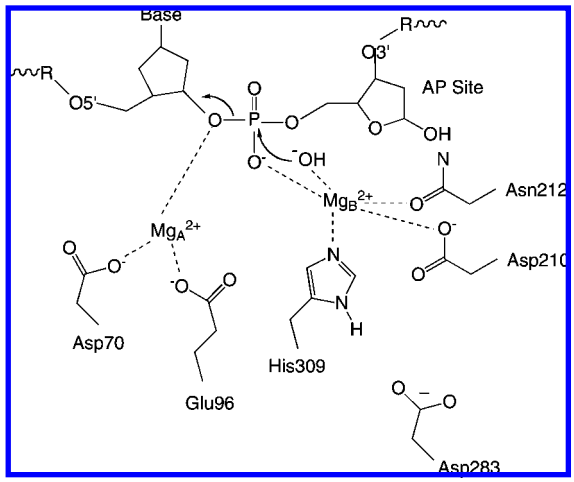

surrogate probes for magnesium. The structures of Tainer and co-workers (1BIX,[13] 1DE8,[14] 1DE9,[14] and 1DEW[14]) utilized acidic crystallization conditions—nominally a pH between 6.2 and 6.5—where the enzymatic activity of APE1 is significantly reduced.[15] In all of these structures, platinum, samarium, or manganese was used as a heavy-atom surrogate for the magnesium ion (except 1DE8, which did not have any metal present). The Tainer group had determined the structures of APE1 that could represent pre- and postincision complexes. On the basis of these structures, they proposed a mechanism involving a single metal. The single metal ion coordinated through Asp70 and Glu96 (from now on referred to as site A), plays a role not only in stabilizing the transition-state intermediate but also in stabilizing the O3′ leaving group. The structure of Wilson and Rupp and co-workers[16] (1E9N) utilized crystals formed from a solution at pH 7.5 (optimal for APE1 activity), and they demonstrated the presence of two metals, with Pb^{2+} being used as the heavy atom surrogate in this instance. Wilson and Rupp also obtained a structure with crystals grown at pH 4.5 (1HD7), and in this case, the structure contained only a single Pb^{2+}, which was bound at site A. Wilson and Rupp and co-workers[16] suggested that the single metal site observed under low-pH conditions is an artifact of these crystallization conditions. Two-metal binding is further supported by biochemical assays showing biphasic inhibition curves at pH 7.5.[16] The Wilson and Rupp model for the active site of APE1 is shown in Scheme 1.

Both groups modeled the overall coordination of the Mg^{2+} geometry as an octahedron, and the water described within the context of the model could be either water or hydroxide. The Mg^{2+} at site A (denoted as Mg_A^{2+}) is composed of residues Asp70, Glu96, and four water ligands (not shown for clarity), and site B (denoted as Mg_B^{2+}) consists of Asn212, Asp210, His309, and three water or hydroxide ligands (again not shown). This second site is closer to the scissile phosphate and would likely stabilize the hydroxyl ion that is proposed to act as the nucleophile.[16] It should be emphasized that both the Tainer and Wilson−Rupp structures support the nature of the metal binding site A.

The Wilson−Rupp scheme formed the basis of a novel mechanism of action of APE1 recently proposed by Oezguen et al.[17] In this mechanism they suggest that a single Mg^{2+} shuttles between sites A and B. The positions of the A and B sites based upon the molecular dynamics (MD) simulations are not much different than those depicted in Scheme 1. The details of how the shuttle is accomplished are beyond the scope of the present work. However, the occupancy of the end-states, and as a result the validity of this model, can be addressed by the experiments described herein.

Because the X-ray data supporting the specific locations for the Mg^{2+} sites uses surrogate probes, the occupancy or existence of site B is still under debate. Further, if site B exists for Mg^{2+}, its coordination environment is uncertain: does the Mg^{2+} coordinate His309? Although not an unusual coordination environment for Pb^{2+}, it is uncommon for Mg^{2+} to be directly bonded to a histidine. Hence, there are questions of both Mg^{2+} stoichiometry and the metal coordination environment for the APE1 endonuclease. The present paper addresses the issues of stoichiometry, and where appropriate we will discuss the nature of the Mg^{2+} coordination environment.

Historically, the only reliable method for characterization of magnesium sites in proteins has been through X-ray crystallography. The X-ray crystallography of magnesium-containing proteins has a complication in that it is often difficult to distinguish Mg^{2+} from Na^+ and/or O^{2-} in modest-resolution protein structures due to the isoelectronic nature of the species. Furthermore, positional disorder and incomplete site occupancy can lead to confusion between disordered water and the presence of Mg^{2+}. To circumvent these issues, many Mg^{2+}-dependent proteins are crystallized with a surrogate metal such as Mn^{2+} or other divalent metal heavy atoms. Moreover, X-ray methods are still dominant because of the unfavorable spectroscopic properties (Ne closed-shell electron configuration) associated with Mg^{2+}. NMR spectroscopy represents an alternative to X-ray methods to characterize Mg^{2+} sites. The magnetic resonance parameters for Mg^{2+} are sensitive to the nature of bound ligands. Unlike NMR spectroscopy of spin $-^1/_2$ nuclides (e.g., ^{13}C and ^{31}P), where the observables are chemical shifts and indirect coupling constants, the principal observable in a solid-state ^{25}Mg NMR experiment is the quadrupole coupling constant C_q, which is extractable directly from the ^{25}Mg NMR line shape. This coupling constant is directly proportional to the electric field gradient at the nuclide and is given by

$$C_q = q_{zz}\left[\frac{e^2}{a_0^3 h}\right]Q \quad (1)$$

$$C_q = q_{zz}(46.852\ \text{MHz}) \quad (2)$$

Here Q is the quadrupole moment of the nucleus in question and q_{zz} is defined as the largest absolute value of the computed field gradient tensor in the principal axis system (PAS) described by diagonalized field gradient tensor q. The traceless field gradient tensor[18] in its PAS frame can be described in terms of q_{zz} and its asymmetry parameter, η_q

(13) Gorman, M. A.; Morea, S.; Rothwell, D. G.; Fortelle, E. L.; Mol, C. D.; Tainer, J. A.; Hickson, I. D.; Freemont, P. S. *EMBO J.* **1997**, *16*, 6548.
(14) Mol, C. D.; Kuo, C. F.; Thayer, M. M.; Cunningham, R. P.; Tainer, J. A. *Nature* **1995**, *374*, 381–386.
(15) Kane, C. M.; Linn, S. *J. Biol. Chem.* **1981**, *256*, 3405–3414.
(16) Beernink, P. T.; Segelke, B. W.; Hadi, M. Z.; Erzberger, J. P.; Wilson, D. M.; Rupp, B. *J. Mol. Biol.* **2001**, *307*, 1023–1034.
(17) Oezguen, N.; Schein, C. H.; Peddi, S. R.; Power, T. D.; Izumi, T.; Braun, W. *Proteins: Struct., Funct., Bioinf.* **2007**, *68*, 313–323. (published online 11 April 2007)
(18) Cohen, M. H.; Reif, M. G. *Solid State Phys.* **1957**, *5*.

$$|q_{zz}| \geq |q_{yy}| \geq |q_{xx}|$$

$$\eta_q \equiv \frac{q_{xx} - q_{yy}}{q_{zz}} \quad (3)$$

The units for q_{zz} are atomic units, and the factor of 46.852 MHz can be computed if the atomic constants are expressed in cgs units and the value of Q is given as 0.1994×10^{-24} cm^2.[19]

With the advent of high-field NMR magnets, there has been a resurgence in the solid-state NMR spectroscopic characterization of Mg^{2+} sites in glasses[20] and novel materials.[21] Of particular interest to the present discussion are biological applications of ^{25}Mg solid-state NMR spectroscopy. To date the applications have been focused Mg^{2+} binding to cofactors such as ATP[22] or chlorophyll[23] or its models.[24] As expected, the work on chlorophyll pushed the limit of sensitivity at room temperature. The present work builds on these previous efforts by examining the solid-state ^{25}Mg NMR spectroscopy of a ~35 kDa protein in the presence and absence of damaged DNA. As we will demonstrate, solid-state ^{25}Mg NMR spectroscopy affords a unique perspective on the structure and environment of Mg^{2+} in biological systems.

Experimental Methods

APE1 Expression and Purification. Recombinant human APE1 protein was overexpressed from clone pETApe1 as described previously.[25] Terrific Broth (TB) shaken culture containing 50 μg/mL ampicillin was inoculated with BL21(DE3) cells harboring the pETApe1 plasmid from starter cultures and grown at 37 °C in baffled flasks until the optical density (A_{600}) reached 0.7−0.8. At that point, protein expression was induced by addition of isopropyl β-D-thiogalactopyranoside (IPTG) to a final concentration of 1 mM. Incubation was continued for 5 h at 37 °C after induction. The cells were harvested at 9000*g* with an average yield of 5 g of wet cells/L of culture. All subsequent steps were performed at 5 °C or on ice. Approximately 15 g of cells was resuspended in 150−200 mL of buffer A (50 mM Hepes, 50 mM KCl, 5% glycerol, KOH, pH 7.5). Cell lysis was carried out with a French press at 16 000 psi pressure and followed by sonication with a Fisher Scientific 550 sonic dismembrator (10 min total time with a 15 s run and a 5 s break interval). Cell debris was removed by centrifugation at 30000*g* for 40−50 min. The clear supernatant was applied to two columns in series: a Q-Sepharose Fast Flow column (26 mm × 340 mm) followed by an HS50 column (16 mm × 110 mm) at a flow rate of 4−5 mL/min. After sample loading, both columns were washed with 600 mL of buffer A and then the Q-Sepharose column was disconnected. APE1 bound in the HS50 column was eluted with a 50−700 mM KCl gradient at a flow rate of 4−5 mL/min. The fractions of the 280 nm absorption peak were analyzed on SDS−polyacrylamide gels for a 35.4 kDa band corresponding to APE1. Clean APE1 fractions were pooled and then dialyzed extensively in buffer (50 mM Hepes, 50 mM KCl, and 1 mM EDTA) to remove glycerol, elution salts, and metal ions, followed by two runs of dialysis with EDTA-free buffer (50 mM HEPES, 50 mM KCl). Average yield of APE1 was 200 mg out of 15 g of cells. Protein concentration was determined by light absorbance at 280 nm, by use of an extinction coefficient of 55 550 M^{-1} cm^{-1}. The extinction coefficient and the molecular mass of 35 423 Da were calculated by the ExPASy Prot Param tool.[26]

APE1 E96Q/D210N and APE1E96Q Expression and Purification. The E96Q/D210N mutation (APE1 ED or simply ED) was created by site-specific mutagenesis of the pETApe1 plasmid.[27] The pETApe1 ED mutant had poor expression levels in both TB and LB media with IPTG induction. In order to produce sufficient amounts of APE1 ED, an autoinducing medium that allows growth to medium-high densities in shaken cultures was used.[28] In contrast to the ED mutant, the E96Q mutant was expressed well in both TB and autoinducing media. Purification of APE1 ED and APE1 E96Q was the same as for wild-type APE1 protein (see above).

Damaged Abasic DNA and Its Characterization. Complementary oligonucleotides

APE1top
5′ - AATTCACCGGTACC[DSPC]TCTAGAATTCG - 3
3′ - TTAAGTGGCCATGG G AGATCTTAAGC - 5
APE1bottom

were prepared by Sigma−Genosys with an abasic residue (Sigma−Genosys nomenclature DSPC describes the abasic site analogue). An equimolar solution of both oligos was heated to 95 °C and then allowed to slowly cool to form the annealed double-stranded abasic DNA−substrate. Gel-filtration chromatography showed a single peak of the expected mobility (data not shown).

Preparation of NMR Samples. Due to the reactivity of the wild-type protein with the damaged DNA, great care was used to maintain the protein and DNA solutions below 5 °C at all times to prevent hydrolysis. Purified apoprotein was mixed with an equimolar amount of abasic double-stranded DNA in 50 mM KCl, 50 mM Hepes, and 1 mM DTT, pH 7.5, on ice. The protein/DNA complexes were then concentrated and buffer-exchanged by ultrafiltration to 3 mg/mL APE1 in 0.5 mM KCl, 0.5 mM Hepes, and 0.01 mM DTT, pH 7.5, at 4 °C. This process took several hours. Six equivalents of isotopically enriched (98.79%) $^{25}Mg^{2+}$ (purchased from Cambridge Isotopes Laboratories as MgO) was added [as $Mg(NO_3)_2$] and allowed to equilibrate for 5 min on ice with occasional mixing. To reduce the ^{1}H spin−lattice relaxation time, cobalt-substituted carbonic anhydrase (0.1 mass equiv) was added as a dopant[29] and then the protein/DNA/Mg solutions were freeze-dried to remove excess water. Dried samples were resuspended with a small volume of 30% glycerol solution (1% of the volume of the sample prior to freeze-drying) that was allowed to slowly absorb into the dried material, then mixed by repeated gentle stirring in an ice bath and light centrifugation at 4 °C. The preparations were almost completely transparent, dark amber solutions with very little opacity due to undissolved solids. The final salt concentration was calculated to be 50 mM KCl. A portion (200 μL) of the resulting liquid was transferred to a 5 mm × 20 mm NMR tube, sealed, and frozen at −40 °C. An aliquot (5 μL) of the final protein and DNA mixture was analyzed by gel filtration to confirm the formation of a DNA/protein complex. A second 5 μL aliquot was analyzed by HPLC (as described below) to ensure that the DNA was not hydrolyzed. Although unreactive, the samples of the ED and E96Q mutants of APE1 complexed with damaged DNA were prepared in the same way as described above. A similar procedure was employed for samples that did not involve damaged DNA.

HPLC Analysis of APE1 DNA Substrate before and after NMR Analysis. An APE1 sample was prepared with equimolar amounts of a double-stranded DNA substrate containing an abasic site and a 6-fold excess of $^{25}Mg^{2+}$ as described above. Before and

(19) Pyykko, P. *Mol. Phys.* **2001**, *99*, 1617–1629.
(20) Kroeker, S.; Neuhoff, P. S.; Stebbins, J. F. *J. Non-Cryst. Solids* **2001**, *293−295*, 440–445.
(21) Bastow, T. J. *Solid State Commun.* **2002**, *124*, 269–273.
(22) Grant, C. V.; Frydman, V.; Frydman, L. *J. Am. Chem. Soc.* **2000**, *122*, 11743–11744.
(23) Wong, A.; Ida, R.; Mo, X.; Gan, Z. H.; Poh, J.; Wu, G. *J. Phys. Chem.* **2006**, *110*, 10084–10090.
(24) Wu, G.; Wong, A.; Wang, S. N. *Can. J. Chem.* **2003**, *81*, 275–283.
(25) Erzberger, J. P.; Barsky, D.; Scharer, O. D.; Colvin, M. E.; Wilson, D. M. *Nucleic Acids Res.* **1998**, *26*, 2771–2778.
(26) Gill, S. C.; von Hippel, P. H. *Anal. Biochem.* **1989**, *182*, 319–326.
(27) Sambrook, J.; Frisch, E. F.; Maniatis, T. *Molecular Cloning: A Laboratory Manual*, 2nd ed.; Cold Spring Harbor Laboratory Press: Cold Spring Harbor, NY, 1989; pp E.3−E.14.
(28) Studier, F. W. *Protein Expression Purif.* **2005**, *41*, 207–234.
(29) Lipton, A. S.; Wright, T. A.; Bowman, M. K.; Reger, D. L.; Ellis, P. D. *J. Am. Chem. Soc.* **2002**, *124*, 5850–5860.

after the NMR experiment, a portion of this sample was removed and the DNA was phenol-extracted, ethanol-precipitated,[27] and analyzed on an HPLC anion-exchange column (GE Healthcare MonoQ HR 5/5 with 10 mM NaOH and a 0−1 M NaCl gradient) to determine the percentage of incision.

^{25}Mg Solid-State NMR Spectroscopy. In our investigation with APE1, we have employed low-temperature (10 K) solid-state NMR[30,31] utilizing cross polarization[32] (CP) from protons to magnesium and quadrupolar Carr−Purcell−Meiboom−Gill (QCPMG) methods.[33,34] The combination of these approaches helps overcome the consequences of dilution noted above between a model compound and the system of interest. To avoid concomitant ^{1}H relaxation problems at 10 K, we have utilized Co^{2+}-substituted carbonic anhydrase (a paramagnetic dopant) as an efficient means for reducing ^{1}H T_1 values while not altering ^{1}H $T_{1\rho}$ values.[35] Some of the ^{25}Mg data sets were acquired at 9.4 T (24.483 MHz for ^{25}Mg and 399.93 MHz for ^{1}H) on a Varian Infinity Plus spectrometer utilizing a "cryogen-free" cryostat designed and built by Cryogenic Ltd (Action Park Industrial Estate, The Vale, London, W3 7QE, U.K.; www.cryogenic.co.uk). A Cryomech Model PT410 pulse tube is the cryorefrigerator used in the present cryostat. The remaining data sets were obtained on a Varian NMR System (VNMRS) spectrometer operating at 11.74 T (30.620 MHz for ^{25}Mg and 500.200 MHz for the ^{1}H frequency) using a home-built probe and Oxford Spectrostat-49 continuous-flow cryostat operating at 10 K. The ^{1}H RF field strength used for both CP and CW decoupling was 50 kHz with a ^{25}Mg Hartmann−Hahn match of 16.7 kHz and selective π-pulse widths of 20 μs for QCPMG detection.[36–38] A 30 ms contact time was utilized in all of our experiments. When needed, three data sets were acquired with 10 kHz transmitter offsets (+10, 0, and −10) and then reconstructed as previously described in a sky projection.[35] A recycle time of 40 s was used, and a flip-back pulse was employed.[39] In a typical experiment, 2K or 4K transients were accumulated before apodization and subsequent Fourier transformation.[35]

To obtain the NMR spectrum, the sample was transferred from a −40 °C freezer to a container containing powdered dry ice. The sample was then transferred from the dry ice to the NMR probe, which in turn was put into a prechilled (230 K) cryostat. It is estimated that the time required for this transfer was on the order of 1 min. With the sample in the probe, the cryostat temperature was then lowered to 10 K. In this transfer procedure the sample never warmed above 0 °C as monitored by a CERNOX resistor in the probe near the sample.

Simulations. The data were analyzed via the program SIMPSON.[40] Simulations of the NMR spectra were performed on a Beowulf cluster at PNNL (composed of 24-Racksaver Dual Pentium IV 2.4 GHz Xeon nodes and 8-Racksaver Dual Pentium III 1.26 GHz nodes) running the Rocks clustering software and utilizing a gigabit Ethernet connection. The fitting procedure utilized for the experimental lineshape was a standard SIMPLEX algorithm within the program. Initial optimizations were performed with ideal pulses until the final fits, where finite RF pulses were utilized.

(30) Lipton, A. S.; Sears, J. A.; Ellis, P. D. *J. Magn. Reson.* **2001**, *151*, 48–59.
(31) Lipton, A. S.; Heck, R. W.; Sears, J. A.; Ellis, P. D. *J. Magn. Reson.* **2004**, *168*, 66–74.
(32) Pines, A.; Gibby, M. G.; Waugh, J. S. *J. Chem. Phys.* **1972**, *56*, 1776.
(33) Bloom, M.; Sternin, E. *Biochemistry* **1987**, *26*, 2101–2105.
(34) Cheng, J. T.; Ellis, P. D. *J. Phys. Chem.* **1989**, *93*, 2549–2555.
(35) Lipton, A. S.; Wright, T. A.; Bowman, M. K.; Reger, D. L.; Ellis, P. D. *J. Am. Chem. Soc.* **2002**, *124*, 5850–5860.
(36) Larsen, F. H.; Jakobsen, H. J.; Ellis, P. D.; Nielsen, N. C. *J. Phys. Chem. A* **1997**, *101*, 8597–8606.
(37) Larsen, F. H.; Skibsted, J.; Jakobsen, H. J.; Nielsen, N. C. *J. Am. Chem. Soc.* **2000**, *122*, 7080–7086.
(38) Lipton, A. S.; Heck, R. W.; Sears, J. A.; Ellis, P. D. *J. Magn. Reson.* **2004**, *168*, 66–74.
(39) Tegenfeldt, J.; Haeberlen, U. *J. Magn. Reson.* **1979**, *36*, 453–457.
(40) Bak, M.; Rasmussen, J. T.; Nielsen, N. C. *J. Magn. Reson.* **2000**, *147*, 296–330.

Results and Discussion

^{25}Mg is a quadrupolar nuclide with a modest magnetic moment and natural abundance (10.13%). These factors conspire to make the ^{25}Mg NMR experiment difficult due to the inherent low sensitivity of ^{25}Mg. This difficulty is further exacerbated by dilution of the spin in the environment of a protein (mass of 25 Da out of ∼35.5 kDa for APE1 in the absence of further diluents such as DNA, salts, and buffers, etc.). To make the consequences of this dilution concrete, consider the comparison between the simple salt $Mg(OAc)_2 \cdot 4H_2O$ and a single site in the protein APE1. The weight percent of Mg^{2+} in the simple salt is ∼11.6%, whereas the weight percent of a single Mg^{2+} in APE1 is 0.07%. This corresponds to a dilution factor of ∼165 (ignoring the additional consequences of the inclusion of damaged DNA, buffers, etc). By taking advantage of the Boltzmann distribution, we can enhance our sensitivity by performing our experiments at cryogenic temperatures (10 K). The combination of CP/QCPMG further enhances our measurement's signal-to-noise ratio (S/N) such that we can more than make up for the dilution of the Mg^{2+} in the protein. Additionally, unlike solution or room-temperature solid-state NMR experiments, complications due to chemical dynamics/exchange have been mitigated due to the cryogenic temperatures employed. However, any chemical dynamics that were occurring prior to freezing will be represented in the final lineshape.

^{25}Mg NMR Lineshapes. Before we discuss the experimental data, it is essential to illustrate some of the features expected in the experimental lineshapes. Presented in Figure 1 are *simulated* ^{25}Mg lineshapes. This figure is designed to introduce some subtle issues that are encountered in the solid-state NMR of quadrupolar nuclides such as found in the ^{25}Mg NMR data presented later. Figure 1a shows a simulation of a ^{25}Mg QCPMG or spikelet spectrum (using "finite" pulses of 8.333 kHz corresponding to a selective $\pi/2$ pulse width of 10 μs) at 9.4 T with a value for C_q of 2.5 MHz, an asymmetry parameter (η_q) value of 1, and a chemical shift of 0. Superimposed on the spikelet spectrum is an ideal powder lineshape for the same value of C_q and η_q as a visual aid. We will denote this lineshape as being reflective of Mg^{2+} in an environment denoted as site 1. The ideal powder lineshape reflects the envelope of the spikelet lineshape. We draw attention to the three features that are typical of a quadrupole lineshape with η_q of 1.0 (η_q values >0.9 are characteristic of virtually every protein resonance we have observed thus far). First, the intensity of the tray (indicated by the horizontal arrows) on the low-frequency side of the maximum in the lineshape eventually comes to the same intensity as the tray on the high-frequency side of the lineshape. Second, under the condition that η_q is 1, the position of the shoulder relative to the maximum and the intensity of the tray is fixed by the value of the quadrupole coupling constant (which is a direct measure of the electric field gradient). Third, any deviations from this ideal line shape can be indicative of artifacts of the pulse sequence,[31] chemical shift anisotropy, or the presence of another species. The consequences of anisotropic shielding can be probed by examining the potential field dependence of the line shape. Employing finite pulses in the lineshape simulations can simulate the potential of pulse sequence artifacts. Another consequence of the high η_q values is that the outer transitions, for example, $\pm^3/_2$ to $\pm^1/_2$, are resonant with the $\pm^1/_2$ transitions, albeit with lower signal-to-noise. We include the possibility of these outer transitions in our simulations as well. The spikelet spectrum depicted in Figure 1a illustrates the type of deviations that exist between ideal

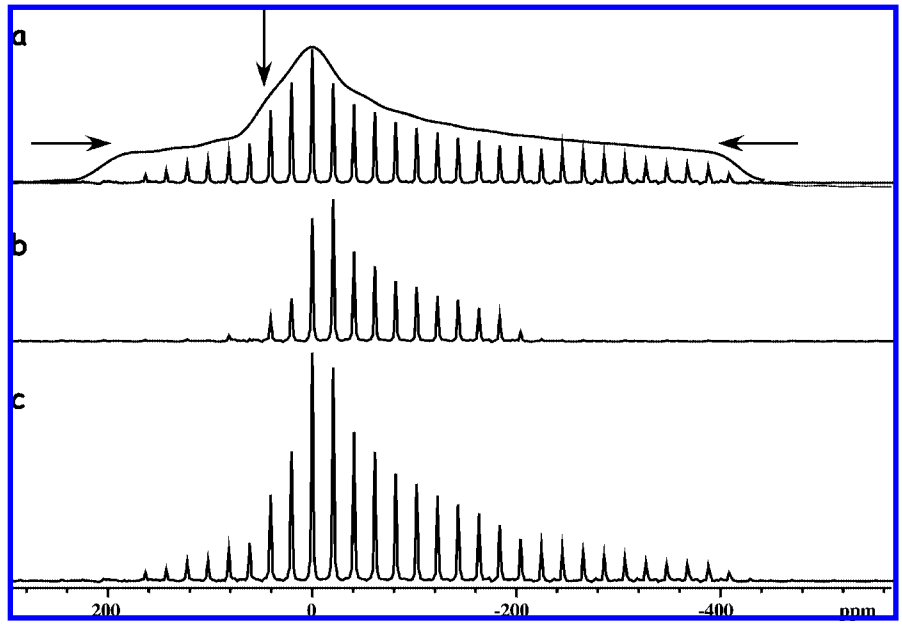

Figure 1. (a) Finite pulse simulation of a ^{25}Mg NMR spikelet lineshape with a quadrupole coupling constant C_q of 2.5 MHz and an asymmetry parameter η_q of 1. Superimposed on the spikelet spectrum is an ideal pulse simulation of a static powder spectrum utilizing the same values of C_q and η_q. The chemical shift of these spectra was arbitrarily set to 0. The horizontal arrows indicate that, under ideal conditions, the heights of the trays on the low- and high-frequency sides of the lineshape are equal. The vertical arrow indicates the position of the shoulder for an $\eta = 1$ line shape. (b) Finite pulse simulation with C_q of 1.7 MHz and an isotropic chemical shift of 12.8 ppm to higher shielding. (c) Sum of spectra a and b such that b is 60% of a. All of the spectra were simulated at 9.4 T.

pulses and finite pulses; namely, loss of intensity at either frequency extreme. Additionally, this loss in intensity can also reflect the change in the CP match condition across the line shape. It is likely that both mechanisms are contributing to the overall loss in intensity. Figure 1b corresponds to Mg^{2+} with a C_q of 1.7 MHz, η_q value of 1, and a chemical shift relative to the Mg^{2+} depicted in Figure 1a of 12.8 ppm (shielded relative to site 1). We denote this lineshape as corresponding to a different environment and label it as site 2.

The spectrum depicted in Figure 1c shows an admixture of the two previous ^{25}Mg spikelet lineshapes; the second site is weighted to be 60% of the first site. Note that what makes the presence of the two different species obvious is that the ratio of the intensities of the tray to the height of the lineshape are wrong for a single site. Additionally, the middle of the lineshape is too broad relative to the height of the trays on either the high- or low-frequency sides of the lineshape.

Figure 1 illustrates how multiple sites would be manifested in the experimental spectrum and is similar to what we find in the present investigation. In the pathological case where there are two sites but each site is reflected by the *same* value of C_q and no difference in chemical shift, we could not detect the difference. We also estimate that if the C_q (and the isotropic chemical shift) of the two sites differed by less than 20%, we could not *meaningfully* detect the difference between the two sites. Distortions from these ideal lineshapes are expected to add to this uncertainty. These discussions are subtle, and as a result we have included a more detailed discussion of these lineshapes in the Supporting Information.

Before we can discuss the specific binding of Mg^{2+} to APE1 in the presence or absence of its substrate DNA, we must address the consequences of nonspecific binding, which is a common attribute of Mg^{2+} chemistry. In the context of the present discussion, nonspecific binding means the binding of Mg^{2+} to any or all sites other than the active site of APE1.

Consequences of Nonspecific Binding. An additional complication associated with ^{25}Mg NMR spectroscopy is the consequences of nonspecific binding, which is the norm for Mg^{2+}-dependent enzymes. Nonspecific binding is rarely an issue in crystallography, but it is a serious one for NMR spectroscopy due to the fact that the NMR experiment "sees" all of the Mg^{2+} in the sample. To overcome this, we have employed a simple difference method[41] where we have constructed a "blank" that we in turn subtract from the spectrum of interest. The blank in this case is a double mutant of APE1 (E96Q/D210N or simply ED) that cannot bind Mg^{2+} in the active site since it lacks important coordinating residues (Scheme 1) yet maintains the ability to bind damaged DNA with an affinity that is ~7 times that of the wild-type APE1.[42]

Binding of Mg^{2+} to APE1 in the Absence of Damaged DNA. Due to the emphasis being on the reaction of a DNA repair protein with damaged DNA, it is often overlooked that Mg^{2+} can bind to the DNA repair protein in the absence of substrate. That is, it is often presupposed that Mg^{2+} binds to the protein when or after the protein has bound the damaged DNA. However, Mg^{2+} could certainly bind to the repair protein in the absence of DNA, given the amount of Mg^{2+} in the nucleus and the comparatively low copy number of the DNA repair proteins. Hence, it is of interest to find out if Mg^{2+} binds to APE1 in the absence of damaged DNA. Figure 2 summarizes the results of such an experiment. The top spectrum (Figure 2a) shows the ^{25}Mg NMR spectrum of wild-type APE1 in the presence of 6 equiv of Mg^{2+}obtained by the methods outlined under Experimental Methods. Figure 2b illustrates the ^{25}Mg NMR spectrum of the ED mutant in the presence of 6 equiv of Mg^{2+}. A cursory visual examination of the data in Figure 2a,b shows that Mg^{2+} binds to APE1 in the absence of DNA; the

(41) Ellis, P. D.; Lipton, A. S. In *Annual Reports in NMR Spectroscopy*; Graham, W., Ed.; Academic Press: San Diego, CA, 2007; Vol. 60.
(42) McNeill, D. R.; Wilson, D. M. *Mol. Cancer Res.* **2007**, *5*, 61–70.

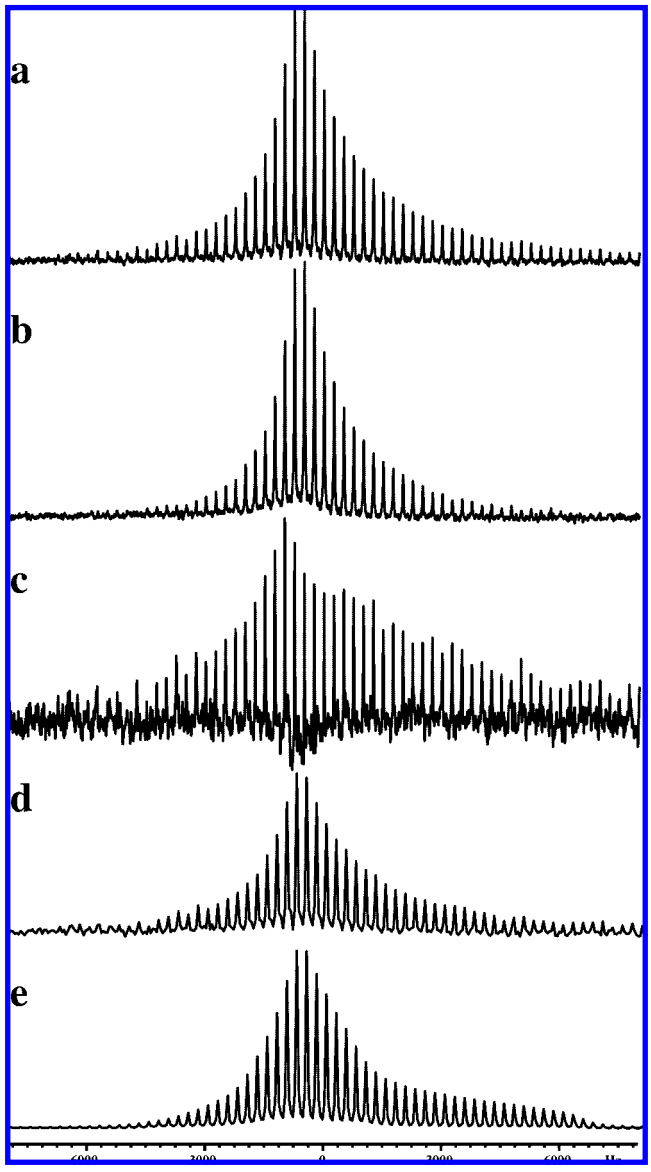

Figure 2. Data at 11.75 T showing the binding of Mg^{2+} to WT APE1 in the *absence* of damaged DNA: (a) ^{25}Mg NMR spectrum of 6X Mg^{2+} bound to APE1; (b) spectrum of 6X Mg^{2+} bound to ED in the *absence* of damaged DNA; (c) oversubtracted difference spectrum; (d) correct difference spectrum. The corresponding fit to the difference spikelet spectrum in (d) shown in (e) utilized the parameters summarized in Table 1.

^{25}Mg spectrum of WT APE1 is broader than the corresponding ^{25}Mg NMR spectrum of the ED mutant. In Figure 2c we have deliberately subtracted too much of the ED spectrum from the spectrum of APE1. This "error" is clearly manifested in a difference spectrum with peaks going below the baseline. This also illustrates one of the boundary conditions for the difference method. The proper difference spectrum is shown in Figure 2d.

The fit of this spectrum (Figure 2e, also see Supporting Information) is consistent with a pair of Mg^{2+} binding sites per mole of APE1 in the absence of DNA with a relative abundance of 1:0.48 (see also Supporting Information). The site with a relative occupancy of 1 will be denoted as site 1 and the other as site 2. If we assume that sites 1 and 2 represent independent sites, with only 6 equiv of Mg^{2+} present and the propensity of Mg^{2+} to bind nonspecifically, then it is unlikely that all of binding site 1 is saturated with Mg^{2+}. Furthermore, if these sites are independent, then this NMR experiment cannot provide information as to whether or not both sites 1 and 2 are occupied *simultaneously*. The details of the quadrupole coupling constants and relative chemical shifts for each site are summarized in Table 1. Briefly, the C_q for site 1 is 2.4 MHz while the C_q for site 2 is 1.3 MHz and the relative chemical shift between the two sites is −2.4 ppm (site 2 being shielded relative to site 1). It is apparent that Mg^{2+} binds to APE1 in the absence of DNA and it is further evident that there are two Mg^{2+} resonances per APE1 molecule.

Table 1. Extracted Values of C_q, η_q, and δ_{iso} for the Mg^{2+} Sites

	C_q (MHz)	η_q	δ_{iso}[a]	weight (%)
		No DNA		
site 1	2.4	0.95		
site 2	1.3	0.79	−2.4	48
		Damaged DNA		
site 1	2.4 (3.2)[b]	0.97 (0.96)[b]		
site 2	1.3 (1.4)[b]	0.98 (1.0)[b]	−25.8 (−28.3)[b]	48 (45)[b]

[a] A negative sign of the chemical shift denotes that site 2 is shielded relative to the Mg^{2+} in site 1. [b] Values in parentheses were determined at 9.4 T (24.483 MHz for ^{25}Mg) on an independently prepared sample. The data was collected with a 500 Hz spike separation as opposed to the optimal 250 Hz spike separation utilized on the 11.74 T spectrometer.

Mg^{2+} Binding to APE1 in the Presence of Damaged DNA. The reactivity of the WT protein when complexed with substrate DNA limits this investigation to a determination of the number of Mg^{2+} sites in APE1. Unpublished data suggested that the reaction would not proceed at a significant rate at temperatures near 0 °C, so sample preparation was dictated by temperature and time constraints. We cannot formally say anything relative to the *equilibrium* binding affinity of one Mg^{2+} site to the other; if the sample were allowed to reach thermodynamic equilibrium at higher temperatures, the reaction would have proceeded before the spectroscopy could be performed. We therefore report only relative site occupancy for a given amount of Mg^{2+} added to the protein/DNA complex at 0 °C. Unlike the first example of APE1 in the *absence* of damaged DNA, there is also the possibility that if a second lineshape is observed, it could arise from the presence of "nicked" DNA (i.e. product DNA, a postreaction state). To address this specific point, we have assayed the sample for nicked DNA after obtaining the NMR data, and those results are summarized in Figure 3. The sample was handled as described under Experimental Methods. HPLC analysis was obtained on aliquots of the NMR sample before and after the low-temperature NMR experiment.

Sample A was extracted before the NMR experiment. Samples B and C were extracted after the NMR experiment, and sample C was incubated at 25 °C for 1 h prior to the DNA extraction to permit incision. The peak at 18.2 mL is the intact APE1 bottom strand of DNA. The 17.7 mL peak is the intact APE1 top strand of DNA with the abasic site. The peaks at 16.3 mL are the products of APE1 hydrolysis of the abasic APE1 top strand of DNA. A brief analysis of the curves shows that approximately 60% of the sample reacted following incubation at 25 °C for 1 h (sample C). This is based on the relative areas of the hydrolyzed strands (the broad peak at 16.3 mL) compared to the area associated with the peak at 17.7 mL (the intact strand).

As the chromatograms depicted in Figure 3 illustrate, to within our experimental error, our protocol summarized above does not allow significant amounts of the APE1 reaction to proceed (<5%; based on chromatograms A and B). Hence, we can obtain NMR data that is reflective of the Mg^{2+} environment within the prereaction complex, and if needed we can allow

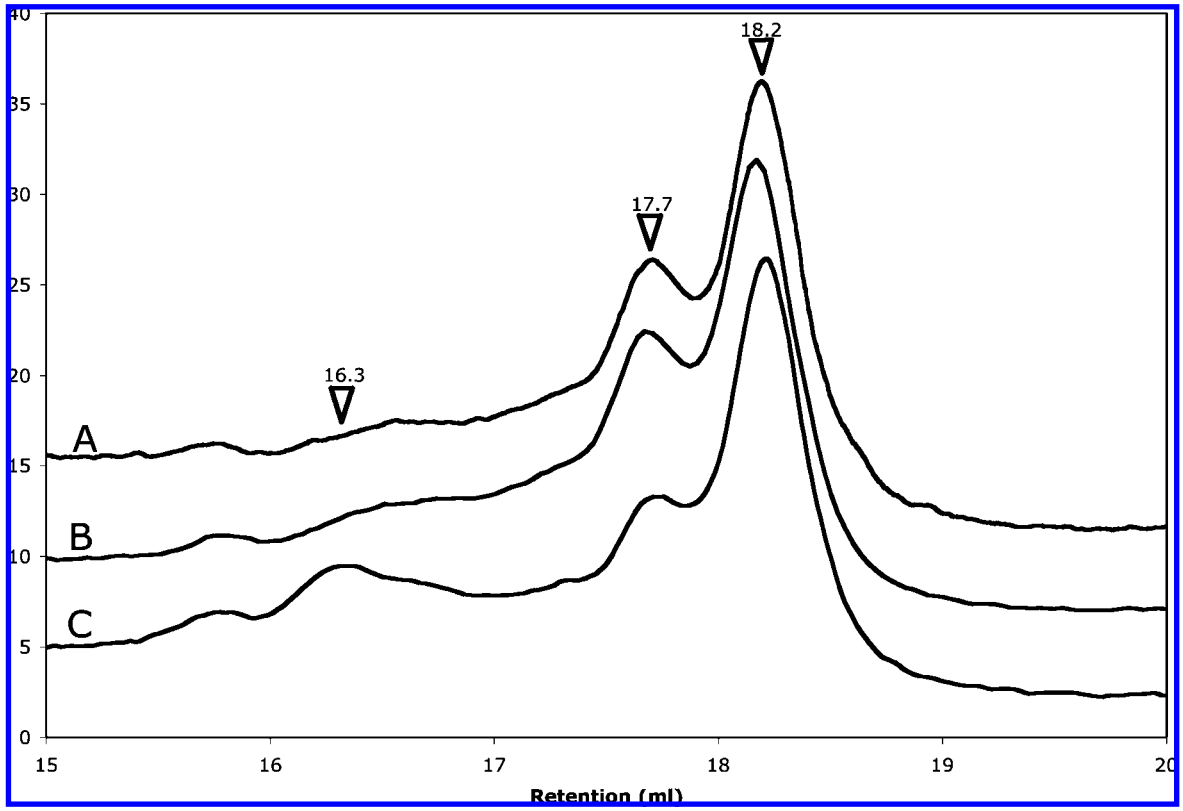

Figure 3. Summary of the results of HPLC analysis on a sample composed of 6 equiv of Mg^{2+}, APE1, and damaged DNA. Sample A was extracted before the start of the NMR experiment; samples B and C were extracted after the NMR experiment. Sample C was incubated at 25 °C for 1 h prior to DNA extraction. The indicators on the chromatograms denote retention volumes at the various peaks' maxima.

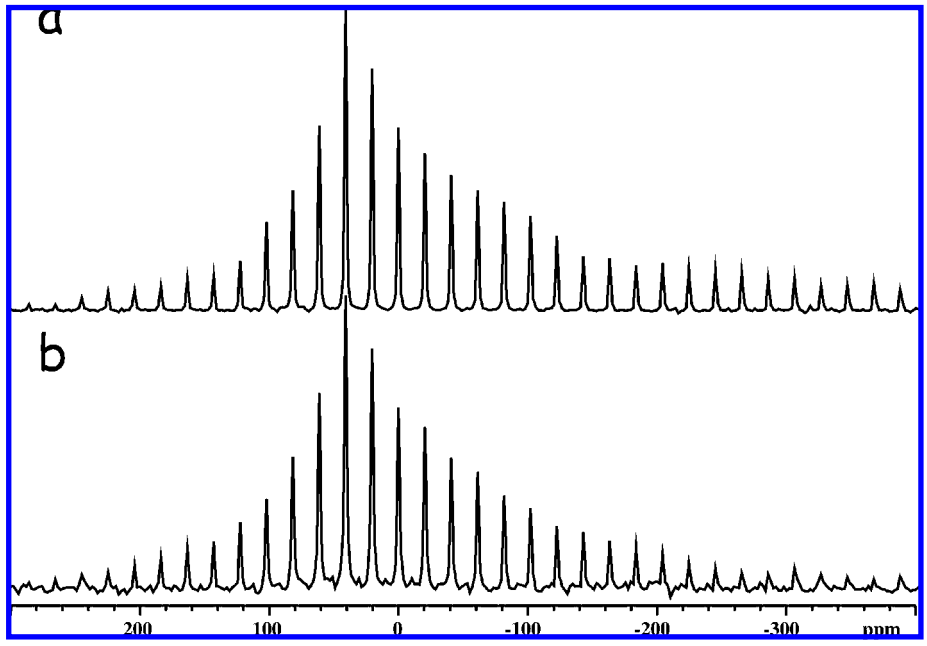

Figure 4. (a) Difference spectrum obtained at 11.75 T that results from the binding of Mg^{2+} to APE1 in the presence of damaged DNA. (b) Corresponding simulation from the extracted parameters listed in Table 1.

the sample to react to obtain analogous data reflecting the Mg^{2+} of the postreaction environment.

Figure 4 shows the resulting difference spectra (utilizing the ED mutant complexed with damaged DNA as a blank) of low-temperature ^{25}Mg NMR experiments for APE1 carried out in the presence of duplex DNA substrate via the procedure described above at 11.75 T. The top spectrum denotes the difference spectrum resulting from the sample (Figure 4a) and its corresponding simulation (Figure 4b) from the extracted parameters. The parameters extracted from that simulation are summarized in Table 1 The spectrum (Figure 4a) could not be fit satisfactorily to single-site occupancy.

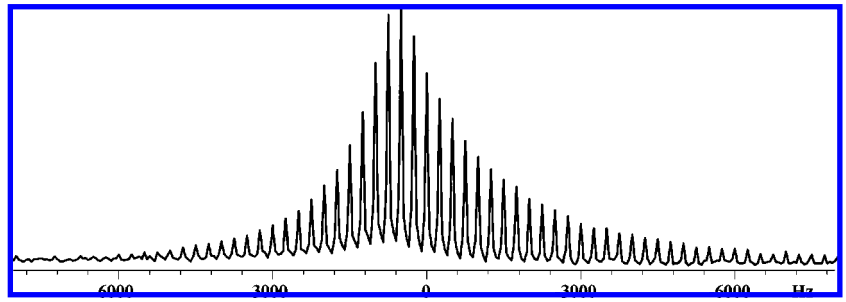

Figure 5. Difference spectrum obtained at 9.4 T resulting from incubating the active APE1/damaged DNA complex for 1 h at 25 °C. See text for details.

However, the spectrum could be simulated by a pair of sites, which was confirmed with different loadings of ^{25}Mg (data not shown). An independently prepared sample was characterized on a 9.4 T spectrometer, and this preparation also showed a second site with similar site occupancy. Even with this similarity, we estimate our experimental error in adding Mg^{2+} ($\sim\pm10\%$), controlling the sample pH ($\sim\pm0.1$ pH unit) in such small volumes, and fitted site occupancy to be on the order of $\pm10\%$. The average values of the NMR parameters summarized in Table 1 are site 1 C_q is 2.4 ± 0.4 MHz, whereas the site 2 C_q is 1.3 ± 0.2 MHz. The isotropic chemical shift reported here is simply the difference between the extracted offsets for the two spectra. The chemical shift of site 2 relative to site 1 (in the *presence* of substrate) is -26.5 ± 3 ppm, site 2 being shielded relative to site 1.

Mg^{2+} in the Postreaction Complex. A sample of WT APE1 and damaged DNA was prepared and allowed to warm to room temperature for 1 h prior to analysis by NMR spectroscopy. The difference spectrum of the postreaction complex is presented in Figure 5. No attempt was made to fit the data. There are several reasons for this; the major one is the complexity of the mixture. Namely, approximately 60% of the material reacted. So we in principle could isolate the spectrum of the postreaction complex by subtracting the remaining 40% of the spectrum of the unreacted material from the experimental spectrum of the postreaction complex. However, given the S/N ratio of the data, the subsequent analysis would still be approximate. What is clear from the breadth of the spectra is that the expected quadrupole coupling constants for the Mg^{2+} product states are not unlike the Mg^{2+} in the reactant complex. Simply stated, the low-temperature ^{25}Mg NMR spectroscopy has the potential to investigate the protein/DNA complex just before and after the incision reaction.

^{25}Mg NMR Spectrum of E96Q Mutant in the Presence of Damaged DNA. It is evident at this point that, in both the absence and presence of damaged DNA, the ^{25}Mg NMR data can be rationalized in terms of two Mg^{2+} species being present in WT APE1. What is the nature of the two sites? The data can be argued as being consistent with one of two different scenarios: (1) the existence of independent Mg^{2+} binding sites, or(2) the existence of a single site that is disordered.

To distinguish between these two options, we have examined the ^{25}Mg NMR spectroscopy of the E96Q mutant of APE1. Recall that E96 is a critical ligand to site A (the remaining residues are D70 and water ligands) depicted in Scheme 1, and the E96Q mutation prevents Mg^{2+} binding at this site.[43] The results of this experiment are pivotal. After the difference is taken between the results for the E96Q and ED mutants to remove the consequences of nonspecific binding, the resonance that remains must be that corresponding to site B. Hence, this experiment will provide a site assignment. If on the other hand, the difference spectrum is a null, the only interpretation consistent with these data is that site B *does not* exist. After a careful subtraction of the results of ^{25}Mg NMR experiments on the ED mutant complexed with damaged DNA from the E96Q mutant/damaged DNA complex, the difference is a null, as summarized in Figure 6. The top spectrum (Figure 6a) is the ^{25}Mg NMR spectrum of the E96Q mutant of APE1.

The middle spectrum (Figure 6b) is the ^{25}Mg NMR spectrum of the ED mutant. The difference spectrum is depicted in Figure 6c. The null spectrum clearly points to the result that the overall stoichiometry with respect to Mg^{2+} is one per mole of APE1, as predicted by the X-ray work of Tainer and co-workers[14] utilizing Mn^{2+} as a surrogate probe for Mg^{2+}. Hence, the two resonances seen above would arise because of *disorder* at a single Mg^{2+} site. Furthermore, this result significantly weakens the "moving metal" mechanism of Oezguen and co-workers. If site B does not exist, then it is evident that this hypothesis has to be rethought. Moreover, the second site observed by Wilson and Rupp must be due to the artifact of the utilization of Pb^{2+} as a surrogate probe for Mg^{2+}. Further, the disappearance of this site as a result of lowering the pH to 4.5 must have come about as the result of protonating H309, thereby preventing the Pb^{2+} from utilizing H309 as a ligand.

There are also several possible interpretations of the existence of a second species that do not rely on the presence of a second binding site. The first possibility could simply be disorder around the metal binding site due to the addition of the Mg^{2+} at near ice temperatures and subsequent low-temperature freezing. That is, as depicted in Scheme 1, the arrangement of ligands D70 and E96 is cis to one another. However, one could envision an arrangement where D70 and E96 are trans to one another. It is not unreasonable to assume that such geometric isomers would have different NMR parameters. The second alternative could arise because the sample pH, 7.5 ± 0.1, could be near the pK_a of one of the waters bound to Mg^{2+}.

In order to investigate the possibility of being near the pK_a of a water ligand bound to Mg^{2+}, we examined the pH dependence of the ^{25}Mg NMR spectrum of APE1. Shown in Figure 7 are the ^{25}Mg NMR spectra of APE1 at two pH values, pH 8 (top spectrum) and pH 6.5 (middle spectrum).[44] The spectra are similar and are consistent with the presence of two sites (see Supporting Information for more details). Subtraction of the two spectra results in a difference spectrum that is a null given the signal-to-noise ratio (bottom spectrum). Hence, it is

(43) Nguyen, L. H.; Barsky, D.; Erzberger, J. P.; Wilson, D. M. *J. Mol. Biol.* **2000**, *298*, 447–459.

(44) Hu, J. Z.; Wind, R. A. *J. Magn. Reson.* **2003**, *163*, 149–162.

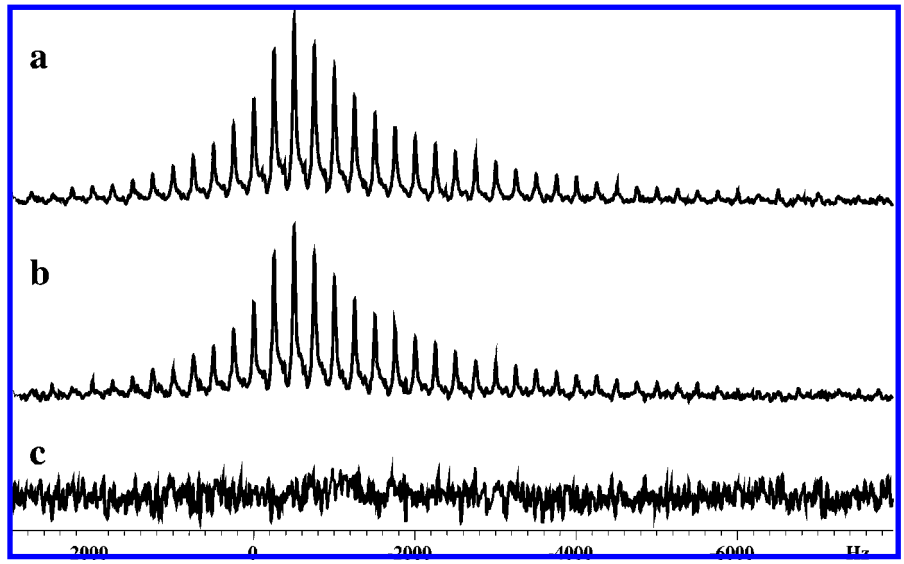

Figure 6. (a) ^{25}Mg NMR spectrum of E96Q damaged DNA complex with APE1. (b) ^{25}Mg NMR spectrum of ED damaged DNA complex. (c) Difference between spectra a and b. All of the data were acquired at 9.4 T.

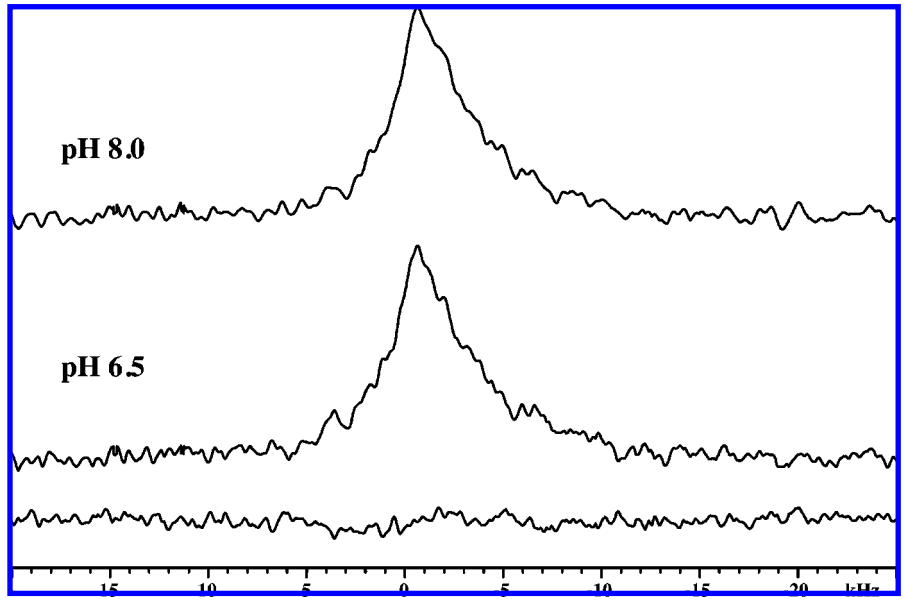

Figure 7. Spectra that result from collapsing the spikelet echo train into a single half-echo and subsequent Fourier transformation. (Top) ^{25}Mg NMR powder spectrum of APE1 at pH 8.0; (middle) ^{25}Mg NMR spectrum of APE1 at pH 6.5; (bottom) difference spectrum formed by subtracting the pH 6.5 spectrum from the pH 8 spectrum. All of the data were acquired at 9.4 T.

evident that the Mg^{2+} in APE1 is not sensitive to a change in pH of 1.5 pH units. If the origin of the two resonances were due to the proximity of a pK_a of a bound ligand, then we should have been able to alter the relative amounts of the two species. Hence, a reasonable explanation for the appearance of the two resonances is the presence of a static disorder of the ligands about the Mg^{2+} coordination sphere. Given that the active site can accommodate a pair of Pb^{2+} (Pb^{2+} having an ionic radius of 1.2 Å)[45] or a single Mn^{2+} (Mn^{2+} has an ionic radius of 0.80 Å)[45] it is not unreasonable with the smaller size of Mg^{2+} (an ionic radius of 0.65 Å)[45] that the ligands around the Mg^{2+} could be arranged differently. Basically, this argues for plasticity of the active site of APE1.

(45) Cotton, F. A.; Wilkinson, G. *Advanced Inorganic Chemistry*, 1st ed.; John Wiley & Sons: New York, 1962.

Summary and Conclusions

By utilizing low-temperature solid-state NMR methods and site-specific mutagenesis, we have determined the number of potential binding sites for Mg^{2+} to the reactive complex between the DNA repair protein APE1 and damaged AP-DNA. It is clear that there is a single specific binding site for Mg^{2+} in a functional APE1/DNA complex. The two resonances reported within represent disorder at site A in Scheme 1 above. At this stage we put forward as a hypothesis that the disorder is due to geometric isomers about the Mg^{2+}. The exact origin of this disorder will have to await an X-ray structure of native APE1 or subsequent modeling. It is critical to point out that these measurements were accomplished with the native metal; that is, a surrogate probe was unnecessary. As concluded here, the use of a surrogate probe can lead to deceptive results. Due to the propensity of Pb^{2+} to chelate nitrogen ligands and the easy

access of H309, a second binding site within APE1 was created. Lowering the pH to 4.5, in all probability, simply protonated H309 and made it unsuitable for metal binding. The present work illustrates that the solid-state NMR experiment in this case provides critical local information about the Mg^{2+} in APE1. In this regard, the solid-state NMR experiment complements the X-ray scattering experiments.

These results are consistent with the mechanism of action of APE1 (binding, recognition, and cleaving damaged DNA) utilizing a single metal cofactor as originally suggested by Tainer and co-workers.[14] This argument is also supported by the ^1H NMR investigations of Lowry et al.[46] They noted that metal titrations (Ca^{2+} and Mg^{2+}) against apo-APE1 only mildly influenced the ^1H resonances corresponding to H309, whereas the addition of Pb^{2+} had dramatic effects on the ^1H H309 resonances. The latter implied that H309 was a direct ligand for Pb^{2+}. Moreover, Lowry et al.[46] concluded that H309 was not a direct ligand for Mg^{2+} (or Ca^{2+}). While not an unusual coordination environment for Pb^{2+}, it is uncommon for Mg^{2+} to be directly bonded to a histidine. Reasoning by analogy to alkaline phosphatase from human placenta, it was possible there was an intervening water molecule between the histidine and the Mg^{2+}.[47,48] However, the ^{25}Mg NMR data of E96Q shows this is not the case; the second binding site is simply not present.

On the basis of molecular dynamics simulations, Oezguen et al.[17] suggested a unique mechanism that involves a single Mg^{2+} going between two binding sites during catalysis. In their simulations these sites are close to the A and B sites observed in the crystallographic experiments that utilized Pb^{2+} as a surrogate probe.[16] Oezguen and co-workers[49] noted that the binding site distance is too large for a typical two-metal mechanism as illustrated with DNA polymerases. Given our experimental results, we argue that the proposed "moving-metal" mechanism cannot be operational. Combining the results discussed here, we note that class II AP endonucleases, such as APE1, execute strand incision via an acid−base reaction platform.

Extensive evidence supports that the primary metal binding site within APE1 and its bacterial homologue, exonuclease III, is site A (composed of residues Asp70, Glu96, and water ligands).[7] The major role for the bound metal ion is likely to position the scissile phosphate bond for hydroxyl-mediated strand cleavage and possibly in stabilizing the leaving-group oxygen.[14,50] In terms of H309, current evidence suggests that this residue, which is essential for APE1 activity, is deprotonated at neutral pH,[46] indicating that H309 likely operates as the Lewis base (in conjunction with D283) to abstract a hydrogen from an active-site water molecule to generate the required attacking nucleophile. Roles for D210 and Y171 in the catalytic reaction are also expected but are currently less clear.[50,51]

Finally, it is evident that the *single* Mg^{2+} site is disordered and appears as two resonances. The resulting C_q differences (averages of 2.4 and 1.3 MHz, respectively) and the observed chemical shift difference will provide experimental metrics for any quantum mechanically derived model of the observed disorder. Those models are being formulated and will provide a rationale as to the nature of the disorder observed at the Mg^{2+} in APE1.

Acknowledgment. We gratefully acknowledge partial support of this work from the National Institutes of Health (Federal Grants EB002050 and EB 003893), by the Department of Energy (DOE) Office of Biological and Environmental Research (OBER) Programs under Grants KP11-01-01: 24931 and 41055, and by the Intramural Research Program of the NIH, NIA. The research was also performed, in part, in the Environmental Molecular Sciences Laboratory (a national scientific user facility sponsored by the DOE OBER) located at Pacific Northwest National Laboratory and operated for the DOE by Battelle.

Supporting Information Available: Details of the analysis of ^{25}Mg solid-state NMR lineshapes of APE1, demonstrating that the line shape is best described as arising from two different Mg^{2+} species in the ratio of 1:0.5. This material is available free of charges via the Internet at http://pubs/acs.org.

JA0776881

(46) Lowry, D. F.; Hoyt, D. W.; Khazi, F. A.; Bagu, J.; Lindsey, A. G.; Wilson, D. M. *J. Mol. Biol.* **2003**, *329*, 311–322.
(47) Murphy, J. E.; Kantrowitz, E. R. *Mol. Microbiol.* **1994**, *12*, 351–357.
(48) Le Du, M. H.; Stigbrand, T.; Taussig, M.; Menez, A.; Stura, E. A. *J. Biol. Chem.* **2001**, *276*, 9158–9165.
(49) Schein, C. H.; Zhou, B.; Oezguen, N.; Mathura, V. S.; Braun, W. *Proteins: Struct., Funct., Bioinf.* **2005**, *58*, 200–210.
(50) Mol, C. D.; Izumi, T.; Mitra, S.; Tainer, J. A. *Nature* **2000**, *403*, 451–456.
(51) Mundle, S. T.; Fattal, M. H.; Melo, L. F.; Coriolan, J. D.; O'Regan, N. E.; Strauss, P. R. *DNA Repair* **2004**, *3*, 1447–1455.